Relativistically corrected electric field gradients calculated with the normalized elimination of the small component formalism

Michael Filatov, Wenli Zou, and Dieter Cremer

Citation: J. Chem. Phys. **137**, 054113 (2012); doi: 10.1063/1.4742175
View online: http://dx.doi.org/10.1063/1.4742175
View Table of Contents: http://jcp.aip.org/resource/1/JCPSA6/v137/i5
Published by the American Institute of Physics.

Relativistically corrected electric field gradients calculated with the normalized elimination of the small component formalism

Michael Filatov,[1,a)] Wenli Zou,[2] and Dieter Cremer[2]
[1]*Mulliken Center for Theoretical Chemistry, Institut für Physikalische und Theoretische Chemie, Universität Bonn, Beringstr. 4, D-53115 Bonn, Germany*
[2]*CATCO group, Department of Chemistry, Southern Methodist University, 3215 Daniel Ave, Dallas, Texas 75275-0314, USA*

(Received 4 June 2012; accepted 19 July 2012; published online 7 August 2012)

Based on the analytic derivatives formalism for the spin-free normalized elimination of the small component method, a new computational scheme for the calculation of the electric field gradient at the atomic nuclei was developed and presented. The new computational scheme was tested by the calculation of the electric field gradient at the mercury nucleus in a series of Hg-containing inorganic and organometallic compounds. The benchmark calculations demonstrate that the new formalism is capable of reproducing experimental and theoretical reference data with high accuracy. The method developed can be routinely applied to the calculation of large and very large molecules and holds considerable promise for the interpretation of the experimental data of biologically relevant compounds containing heavy elements. © *2012 American Institute of Physics*. [http://dx.doi.org/10.1063/1.4742175]

I. INTRODUCTION

The electric field gradient (EFG) at an atomic nucleus is a sensitive property reflecting the local chemical environment in so far as it depends on the non-spherically symmetric part of the electron density distribution of the resonating atom.[1] The EFG can be accessed via the nuclear quadrupole interaction, which can be measured by various experimental techniques, including Mössbauer spectroscopy,[2] nuclear quadrupole resonance spectroscopy,[3,4] or perturbed angular correlations (PAC) of γ-rays spectroscopy.[5] The interpretation of the experimental spectroscopic data often requires high level theoretical calculations to reveal the relationship between the electronic structure and the measured nuclear quadrupole interaction.[6]

A variety of theoretical approaches have been recently applied to the calculation of EFGs in atomic and molecular systems of which only a few can be mentioned here: (i) approaches based on the quasi-relativistic zero-order regular approximation (ZORA) realized for density functional theory,[7] (ii) the direct perturbation theory approach of Stopkowitz *et al.*,[8] (iii) the high-order Douglas-Kroll-Hess (DKH) approximation at the self-consistent field theory level,[9,10] and (iv) the four-component relativistic Dirac-Coulomb formalism in connection with a high level treatment of electron correlation.[11–14] In particular, Pernpointner *et al.*[15] have demonstrated the necessity of the inclusion of relativistic and electron correlation effects into the molecular calculations for obtaining accurate theoretical estimates of the EFG for heavy atoms. This has been recently confirmed by Arcisauskaite *et al.*[14] in high-level four-component calculations on a series of mercury compounds.

Due to the computational complexity, high-level correlated calculations in connection with the four-component Dirac-Coulomb Hamiltonian can only be carried out for small molecules with a few atoms. For the interpretation of the experimental data, theoretical calculations of large and very large molecules are desirable, which requires the development of simple yet accurate theoretical methods. In a series of recent articles,[16–18] we have developed and presented the analytic derivatives formalism for the normalized-elimination of the small component (NESC) relativistic method.[19] The formalism developed[20] has been applied to the calculation of analytic energy gradients in geometry optimizations,[16] the calculation of contact densities at the nuclei of heavy atoms,[17] and the calculation of the isotropic hyperfine structure constants,[18] vibrational frequencies and electric polarizabilities for compounds of heavy elements.[21] These applications have verified the high accuracy of the NESC formalism developed, its conceptual and computational simplicity, and its applicability when investigating large and very large molecules. In the present work, the NESC analytic derivatives formalism will be extended to the calculation of the electric field gradient. It will be tested in the calculation of EFGs for the mercury nucleus in a series of inorganic and organometallic compounds of Hg. The development of this formalism should provide a possibility of routinely calculating EFGs in large inorganic, organometallic, and bio-inorganic compounds containing heavy elements.

II. THEORY

The interaction of the nuclear quadrupole moment (NQM) Q_{ij} with the electric field gradient (EFG) V_{ij} at the site of the nucleus is described by Eq. (1),[1,22]

$$\hat{H}^{int} = \sum_{i,j} Q_{ij} V_{ij}, \tag{1}$$

a)Electronic mail: mike.filatov@gmail.com.

where the summation is carried out with respect to the Cartesian components $i, j = x, y, z$. Usually, the NQM tensor components are expressed in terms of the nuclear spin operator as in Eq. (2),

$$Q_{ij} = \frac{eQ}{2I(2I-1)}\left(\frac{1}{2}\left(\hat{I}_i\hat{I}_j + \hat{I}_j\hat{I}_i\right) - \frac{1}{3}\delta_{ij}I(I+1)\right), \quad (2)$$

where I and $\hat{I}_i$ are the nuclear spin and the nuclear spin operator, respectively; Q is the nuclear quadrupole moment, and e is the electron charge. Note that, for nuclei with $I = 1/2$, all components Q_{ij} of the NQM tensor vanish.

For a given nucleus, the EFG operator, see Eq. (3), is defined as a second derivative with respect to the Cartesian coordinates

$$V_{ij} = \left(\frac{\partial}{\partial x_i}\frac{\partial}{\partial x_j} - \frac{1}{3}\delta_{ij}\nabla^2\right)V, \quad (3)$$

of the electrostatic potential V, which describes interaction of a given nucleus with electrons and other nuclei in the molecule. The EFG defined in this way is a symmetric traceless tensor as requested by the Laplace equation. Often, it is convenient to define the principal axis system (by diagonalization of the V_{ij} tensor), in which the principal axes a, b, and c are labeled such that the diagonal components V_{aa}, V_{bb}, and V_{cc} satisfy the relation $|V_{aa}| \le |V_{bb}| \le |V_{cc}|$. Then, the EFG tensor can be characterized by only two parameters, the principal value V_{cc} and the asymmetry parameter $\eta = (V_{aa} - V_{bb})/V_{cc}$. In practice, a nuclear quadrupole coupling constant (NQCC) ν_Q, Eq. (4),[1,3,23] is used to interpret nuclear quadrupole resonance (NQR) and Mössbauer spectra,[2,4]

$$\nu_Q = \frac{eQ\langle V_{cc}\rangle}{h}, \quad (4)$$

in which $\langle V_{cc}\rangle$ is the expectation value of the V_{cc} EFG operator in the ground electronic state of the molecule.

A. NESC electric field gradient

In the context of a quantum chemical method that satisfies the Hellmann-Feynman theorem[24,25] (e.g., the Hartree-Fock method), the expectation value of an operator that perturbs the molecular Hamiltonian can be obtained by differentiating the total energy of the perturbed system with respect to the perturbation parameter(s). Adding the nuclear quadrupole interaction Hamiltonian (1) to the potential energy operator of the NESC Hamiltonian[19,26] and differentiating the resulting total energy $E^{\mathrm{NESC}}(Q_{ij}^K)$ with respect to the components of NQM Q_{ij}^K yields the corresponding EFG expectation values at the position of the Kth nucleus as defined by Eq. (5),

$$\langle V_{ij}^K\rangle = \left.\frac{\partial E^{\mathrm{NESC}}(Q_{ij}^K)}{\partial Q_{ij}^K}\right|_{Q_{ij}^K\to 0} \quad (5a)$$

$$+\sum_{L\neq K} Z_L \frac{3X_{i,KL}X_{j,KL} - \delta_{ij}R_{KL}^2}{R_{KL}^5}, \quad (5b)$$

where the term in Eq. (5b) represents the nuclear-nuclear part of the EFG and $X_{i,KL}$ are the Cartesian components of the internuclear distance vector $\mathbf{R}_{KL} = \mathbf{R}_K - \mathbf{R}_L$. Note that, when calculating the NESC electronic energy $E^{\mathrm{NESC}}(Q_{ij}^K)$ in Eq. (5a), only the electron-nuclear interaction potential should be used in connection with Eq. (3).

In the NESC method,[19] the exact relativistic one-electron Hamiltonian[27] is projected onto the positive-energy (electronic) states and renormalized on the non-relativistic metric thus yielding the Newton-Wigner representation.[28,29] In many-electron calculations, the spin-free NESC one-electron Hamiltonian obtained in this way replaces the usual non-relativistic one-electron Hamiltonian (the sum of the kinetic and the nuclear-electron attraction potential energy operators) thus leading to an accurate account of the major part of the scalar-relativistic correction to the electronic energy.[26] As has been shown by Dyall,[19,26] only a tiny fraction of the scalar-relativistic Dirac-Coulomb energy[30,31] of a many-electron system in form of the renormalized two-electron Darwin term is lost in the spin-free one-electron NESC method.

The nuclear quadrupole interaction (1) perturbs the nuclear-electron attraction energy, which enters the one-electron NESC Hamiltonian via the matrices of the operators $V(\mathbf{r}) = -\sum_K Z_K v(\mathbf{r}-\mathbf{R}_K)$ and $W(\mathbf{r}) = (\boldsymbol{\sigma}\cdot\mathbf{p})V(\mathbf{r})(\boldsymbol{\sigma}\cdot\mathbf{p})/4m^2c^2$. In these operators, $v(\mathbf{r}-\mathbf{R}_K)$ is the Coulomb potential of a point-like or a finite-size charge distribution of the Kth nucleus, Z_K is the nuclear charge, $\boldsymbol{\sigma} = \{\sigma_x, \sigma_y, \sigma_z\}$ is a vector of the Pauli matrices, $\mathbf{p}$ is the linear momentum operator, m is the electron mass, and c is the velocity of light.

The derivative of the NESC total molecular energy with respect to the perturbation parameters can be obtained using the NESC first derivatives formalism developed in our previous works (see Refs. 16–18). Using Eqs. (15) and (16) from Ref. 18, the derivatives in Eq. (5) are given by Eq. (6)

$$\frac{\partial E^{\mathrm{NESC}}(Q_{ij})}{\partial Q_{ij}^K} = tr\left(\tilde{\mathbf{P}} + \mathbf{P}_{0V} + (\mathbf{P}_{0V})^\dagger\right)\frac{\partial \mathbf{V}}{\partial Q_{ij}^K} \quad (6a)$$

$$+tr\left(\mathbf{U}\tilde{\mathbf{P}}\mathbf{U}^\dagger + \mathbf{P}_{0W} + (\mathbf{P}_{0W})^\dagger\right)\frac{\partial \mathbf{W}}{\partial Q_{ij}^K}, \quad (6b)$$

where $\mathbf{U}$ is the matrix of the elimination of the small component operator[19] and the matrices $\tilde{\mathbf{P}}$, $\mathbf{P}_{0V}$, and $\mathbf{P}_{0W}$ are obtained from the usual molecular density matrix as described in Refs. 17 and 18. In these matrices, the effect of renormalization from the Dirac-Pauli representation of relativistic equations to the Newton-Wigner representation (sometimes called the picture change effect) is correctly taken into account along with the effect resulting from the decoupling between the electronic and positronic states.[17,18] It has to be noted that no approximations are made in Eq. (6), which yields the exact derivative of the NESC total energy.

The derivatives $\frac{\partial \mathbf{V}}{\partial Q_{ij}^K}$ and $\frac{\partial \mathbf{W}}{\partial Q_{ij}^K}$ entering Eq. (6) can be obtained as the second derivatives of the respective molecular integrals with respect to nuclear coordinates. Differentiation of Eq. (7),

$$\mathbf{V}(Q_{ij}^K) = \left\langle \chi_\mu \middle| V(\mathbf{r}) + \sum_{i,j} Q_{ij}^K V_{ij}^K \middle| \chi_\nu \right\rangle, \quad (7)$$

where χ_μ and χ_ν are the basis functions, with respect to Q_{ij}^K yields Eq. (8).

$$\frac{\partial \mathbf{V}(Q_{ij}^K)}{\partial Q_{ij}^K} = \left\langle \chi_\mu \left| V_{ij}^K \right| \chi_\nu \right\rangle, \tag{8a}$$

$$= \left\langle \chi_\mu \left| \left(\left(\frac{\partial}{\partial x_i} \frac{\partial}{\partial x_j} - \frac{1}{3}\delta_{ij}\nabla^2 \right) v(\mathbf{r} - \mathbf{R}_K) \right) \right| \chi_\nu \right\rangle, \tag{8b}$$

$$= \left(\frac{\partial^2}{\partial X_{i,K} \partial X_{j,K}} - \frac{1}{3}\delta_{ij}\nabla_K^2 \right) \left\langle \chi_\mu \left| v(\mathbf{r} - \mathbf{R}_K) \right| \chi_\nu \right\rangle. \tag{8c}$$

When converting Eq. (8b) to Eq. (8c), it is used that the interaction potential $v(\mathbf{r} - \mathbf{R}_K)$ depends on the electron-nuclear distance $\mathbf{r} - \mathbf{R}_K$ and, therefore, differentiation with respect to $\mathbf{r}$ is equivalent to differentiation with respect to $-\mathbf{R}_K$ (see Ref. 32). Note that, in Eq. (8c), only the interaction potential should be differentiated with respect to the Cartesian components $X_{i,K}$ of the vector $\mathbf{r} - \mathbf{R}_K$.

Using the Gaussian function to model the nuclear charge distribution, the electron-nuclear interaction potential $v(\mathbf{r} - \mathbf{R}_K)$ is given by Eq. (9),

$$v(\mathbf{r} - \mathbf{R}_K) = -\frac{1}{|\mathbf{r} - \mathbf{R}_K|} erf\left(\frac{|\mathbf{r} - \mathbf{R}_K|}{\zeta_K} \right), \tag{9}$$

where *erf* is the error function and ζ_K is the parameter related to the root mean square (rms) charge radius $\langle R_K^2 \rangle^{1/2}$ of the nucleus K as in Eq. (10),

$$\zeta_K = \sqrt{\frac{2}{3}} \langle R_K^2 \rangle^{1/2}. \tag{10}$$

Note that setting $\zeta_K = 0$ recovers the usual Coulomb potential of a point charge.

The molecular integrals $\langle \chi_\mu | v(\mathbf{r} - \mathbf{R}_K) | \chi_\nu \rangle$ can be calculated using the formalism developed by Taketa *et al.*[33] When calculating the derivatives $\frac{\partial \mathbf{W}(Q_{ij}^K)}{\partial Q_{ij}^K}$, the latter integral is replaced by $\langle (\boldsymbol{\sigma} \cdot \mathbf{p}) \chi_\mu | v(\mathbf{r} - \mathbf{R}_K) | (\boldsymbol{\sigma} \cdot \mathbf{p}) \chi_\nu \rangle$ or, in the spin-free approximation (i.e., neglecting the spin-orbit coupling), by $\langle \nabla \chi_\mu | v(\mathbf{r} - \mathbf{R}_K) | \cdot \nabla \chi_\nu \rangle$. The derivatives in Eq. (6) are formulated entirely in terms of traces of matrix products and the practical application of these formulae requires only a fraction of time needed for a single Hartree-Fock (HF) iteration.

III. COMPUTATIONAL DETAILS

The formalism described in Sec. II was implemented in the COLOGNE2011 suite of programs.[34] When using the finite-size nuclear model, the values of the rms nuclear charge radii of all the elements were taken from the compilation of Visscher and Dyall.[35] For a point charge nucleus model, the value of the ζ parameter in Eq. (9) was set to zero. In the relativistic calculations, the value $c = 137.035999070(98)$ a.u.[36] was used for the velocity of light. The non-relativistic calculations were carried out using the same computer code by setting the velocity of light to 10^8 a.u.

The open-shell species were calculated using the spin-unrestricted formalism. When calculating the EFG values, all electrons were correlated in the post-Hartree-Fock methods. The spin-free formalism was used throughout this work.

TABLE I. Electric field gradients V_{cc} (in a.u.) calculated for hydrogen halides HX (X = F, Cl, Br, I, At) using the HF method. Basis sets and molecular geometries are taken from Ref. 10. The point charge nucleus model is used.

Molecule	sf-DC-HF[a]	NESC/HF	DKH7/HF[b]	HF[c]
HF	2.809762	2.809268	2.809266	2.799747
HCl	3.591413	3.590266	3.590207	3.541602
HBr	7.542301	7.536883	7.536523	7.009479
HI	11.640837	11.628164	11.627166	9.670471
HAt	26.755285	26.702020	26.690805	15.358366

[a]Spin-free Dirac-Coulomb Hartree-Fock calculations taken from Ref. 37.
[b]Seventh order Douglas-Kroll-Hess calculations from Ref. 10.
[c]Non-relativistic HF calculations; this work.

IV. RESULTS

The formalism described in Sec. II has been tested in the calculation of EFGs for a set of hydrogen halides HX (X = F, Cl, Br, I, At). In these calculations, the geometries of hydrogen halides were taken from Ref. 10 as well as the basis sets for all atoms. In Table I, the results of the NESC/HF calculations carried out with the use of the point charge nucleus model (i.e., setting $\zeta = 0$ in Eq. (9)) are compared with the results of the spin-free Dirac-Coulomb Hartree-Fock (sf-DC-HF) calculations from Ref. 37, high-order (DKH7) Douglas-Kroll-Hess (DKH) calculations,[10] and non-relativistic HF results. All calculations reported in Table I employ the same basis set.[10]

Although the NESC method is computationally much simpler than the high-order DKH approach (in the latter method, the energy calculation alone requires thousands of matrix multiplications[38]), the NESC EFG values reported in Table I are closer to the reference values obtained with the sf-DC-HF calculations. The remaining deviation of the NESC EFG values from the reference sf-DC-HF values is attributed to the effect of the two-electron Darwin terms neglected in the one-electron NESC method.[19,26] However, even for an element as heavy as astatine, the effect of the neglected two-electron terms is less than 0.2% and is much less than the total relativistic correction to the calculated EFG (~43%). We note that the inclusion of the neglected two-electron terms into the NESC calculations would have required the calculation of a large number of additional two-electron integrals thus leading to a considerable increase of computational costs without noticeable gain in accuracy.

In Table II, the results of NESC/HF and NESC/MP2 calculations carried out utilizing the finite nucleus model are compared with the reference data obtained from four-component Dirac-Coulomb HF calculations.[10] Comparison of the NESC/HF and the 4c-DC-HF EFG values reveals the effect of the spin-orbit coupling (SOC) interactions. For the heaviest hydrogen halide HAt, SOC leads to a reduction of V_{cc} of ~2% . As the elements at the end of a period in the periodic table have the largest SOC effects, this result indicates

TABLE II. Electric field gradients V_{cc} (in a.u.) calculated for hydrogen halides HX (X = F, Cl, Br, I, At) using the NESC/HF and NESC/MP2 methods. The basis sets and molecular geometries are taken from Ref. 10. The finite size nucleus model is used.

Molecule	4c-DC-HF[a]	NESC/HF	NESC/MP2
HF	2.809754	2.809268	2.554123
HCl	3.591314	3.590261	3.402235
HBr	7.540289	7.536556	7.254653
HI	11.623332	11.620941	11.047529
HAt	25.979844	26.506524	26.273005

[a]Four-component Dirac-Coulomb Hartree-Fock calculations taken from Ref. 10.

TABLE III. Electric field gradients V_{cc} (in a.u.) calculated for a set of HgX_2 (X = Cl, Br, I, CH_3) compounds. The molecular geometries are taken from Ref. 14. The uncontracted QZ basis set as described in Ref. 14 is used for all atoms.

Molecule	4c-DC-HF[a]	NESC(fn)/HF[b]	NESC(pn)/HF[c]
$HgCl_2$	−12.95	−12.14	−12.12
$HgBr_2$	−11.82	−11.11	−11.09
HgI_2	−11.68	−11.04	−11.03
$Hg(CH_3)_2$	−19.83	−18.77	−18.78

[a]Four-component Dirac-Coulomb Hartree-Fock calculations with unrestricted kinetic balance condition taken from Ref. 14.
[b]Finite nucleus model used.
[c]Point-charge nucleus model used.

that SOC plays only a minor role for the correct calculation of the EFG, especially in the case of lighter elements.

Comparing the NESC/HF data in the third column of Tables I and II reveals that using the finite size nucleus model leads to a minute decrease of the absolute value of V_{cc} (∼0.7% for HAt). The effect of using the finite size nucleus rapidly disappears as the atomic number of the halogen atom decreases. Electron correlation plays a more important role for the calculated EFGs, especially for lighter atoms. Inclusion of electron correlation leads to a reduction of the absolute value of V_{cc}, which varies between ∼10% for HF and 0.9% for HAt. The inclusion of electron correlation at the relativistic level causes an increase of the electron density in the K-shell and depletion of the density in the higher lying shells.[39] As the EFG depends on the non-spherically symmetric (quadrupole) part of the electron density, this depletion may lead to a reduction of its absolute magnitude.

The performance of the NESC method has been further investigated in the calculation of EFGs for a series of mercury compounds. In Table III, the results of the NESC/HF calculations carried out with the use of the point charge nucleus model and with the use of the finite nucleus model are compared with the results of 4c-DC-HF calculations from Ref. 14. These calculations are carried out with the use of a very large uncontracted basis set of quadruple-zeta (QZ) quality as described in Ref. 14. As the major difference between the reference 4c-DC-HF and the NESC/HF calculations results from the absence of the SOC effects in the latter, the data of Table III confirm that SOC plays only a minor role for the EFG values contributing a mere few percent into the final value. Furthermore, the effect of finite size nucleus model in the NESC/HF calculations is negligibly small, even for an element as heavy as mercury.

The EFG values V_{cc} as well as the effective contact densities,[17] $\Delta\bar{\rho} = \bar{\rho}_{\mathrm{Hg}} - \bar{\rho}_{Mol}$, for the mercury atom were calculated for an extended set of mercury molecules listed in Table IV. Beside the compounds from Ref. 14, a number of other molecules studied recently by us[17] was included into the calculations. In addition, two Hg(II) complexes, $Hg(cys)_2$ and $HgCl_2$-crown-S_6, were studied. The geometries of $HgCl_2$, $HgBr_2$, HgI_2, $Hg(CH_3)_2$ were taken from Ref. 14, the geometries of HgF, HgF_2, HgF_4, $Hg(SH)_4^{2-}$, and $Hg(SH)_4$ were taken from Ref. 17, and the geometries of Hg(II)-L-cysteine, $Hg(cys)_2$,[40] and $HgCl_2$-crown-S_6 ((Z,Z,Z,Z,Z,Z)-1,4,7,10,13,16-hexathiacyclooctadeca-2,5,8,11,14,17-hexaene,[41,42] see Figure 1) were optimized using the NESC/B3LYP method. In the geometry optimizations, the segmented all-electron relativistically contracted (SARC)

TABLE IV. Electric field gradients V_{cc} (in a.u.) and effective contact densities $\bar{\rho}$ (in bohr^{-3}) calculated for a set of mercury compounds. The molecular geometries are taken from Refs. 14, 47, and 17. The modified SARC basis set (see text) is used for mercury and the TZVPP basis set is used for other elements.

			NESC/HF		NESC/MP2		4c-DC-CCSD-T[b]
Entry[a]	Molecule	Symmetry	V_{cc}	$\Delta\bar{\rho}$[c]	V_{cc}	$\Delta\bar{\rho}$	V_{cc}
1	HgF	$C_{\infty v}$	−8.68 (−8.45)[d]	96.64	− 5.78	80.72	
2	HgF_2	$D_{\infty h}$	−12.85 (−12.55)	119.70	− 9.18	108.00	
3	HgF_4	D_{4h}	+4.40 (+4.44)	95.17	+3.74	109.38	
4	$HgCl_2$	$D_{\infty h}$	−12.40 (−12.14)	110.05	− 9.32	98.15	− 9.51
5	$HgBr_2$	$D_{\infty h}$	−11.31 (−11.11)	111.66	− 8.54	97.26	− 8.63
6	HgI_2	$D_{\infty h}$	−11.17 (−11.04)	101.51	− 8.64	85.53	− 8.61
7	$Hg(CH_3)_2$	D_{3h}	−19.30 (−18.77)	49.04	− 15.22	45.11	− 15.71
8	$Hg(SH)_4$	C_{4h}	+8.00	87.57	+4.99	85.39	
9	$Hg(SH)_4^{2-}$	S_4	+0.84	162.03	+0.82	149.40	
10	$Hg(cys)_2$[e]	C_1	−13.23	86.72	− 9.38	72.72	
11	$HgCl_2$-crown-S_6[e]	C_{6v}	−9.87	144.31	− 7.28	126.77	

[a]Number of entry in Figure 2.
[b]Taken from Ref. 14.
[c]Calculated with respect to the contact density for a neutral mercury atom, $\Delta\bar{\rho} = \bar{\rho}_{\mathrm{Hg}} - \bar{\rho}_{Mol}$ ($\bar{\rho}_{\mathrm{Hg}}^{\mathrm{HF}}$=2106192.35 bohr^{-3}, $\bar{\rho}_{\mathrm{Hg}}^{MP2}$=2106301.66 bohr^{-3}).
[d]Values in parentheses obtained using completely uncontracted QZ basis set.
[e]Geometry optimized in this work using NESC/B3LYP with SARC and TZVPP basis sets.

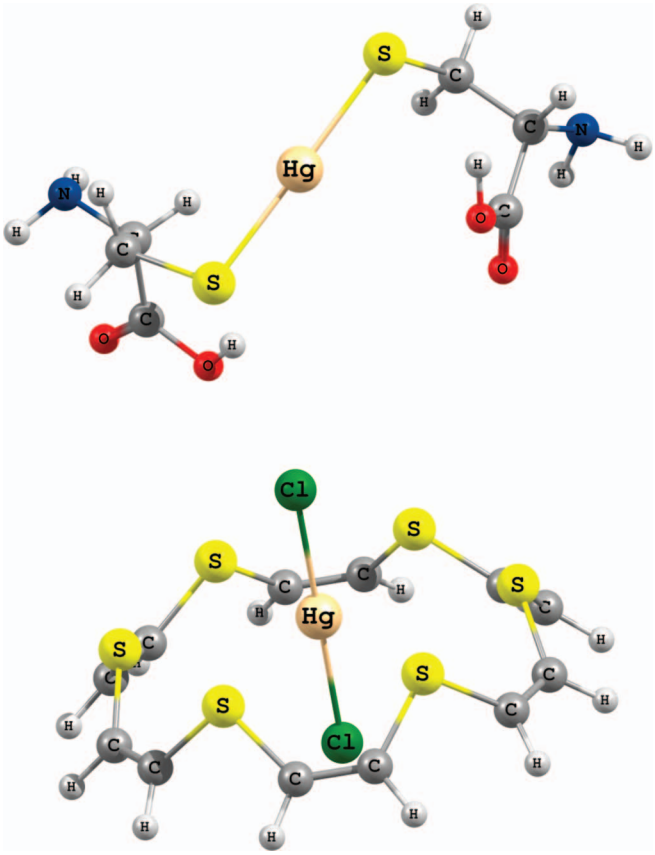

FIG. 1. Geometries of $Hg(cys)_2$ (upper panel) and $HgCl_2$-crown-S_6 (lower panel) molecules.

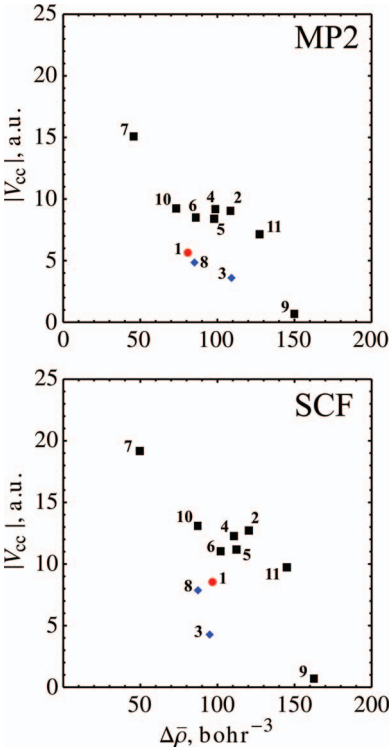

FIG. 2. Electric field gradient V_{cc} (in a.u.) vs. the effective contact density $\Delta\bar{\rho} = \bar{\rho}_{Hg} - \bar{\rho}_{Mol}$ (in $bohr^{-3}$) for mercury compounds calculated using the NESC/HF method (lower panel) and the NESC/MP2 method (upper panel). Black squares label the Hg(II) compounds, red dot the Hg(I) compound, and blue diamonds the Hg(IV) compounds.

basis set[43] was used for mercury combined with the 6-31+G(d) basis set[44] for other elements.

When calculating the EFGs and effective contact densities of the molecules of Table IV, the SARC basis set was modified as follows. The two tight-most primitive functions in the contracted s-type basis function were uncontracted and five tight primitive functions were added in a geometric progression.[17] Two tight primitive p-type functions and two tight primitive d-type functions with the exponents obtained from a geometric progression were added to the set of p- and d-type basis functions. The augmented SARC basis set on mercury was combined with the all electron def2-valence triple-zeta basis functions with three sets of first polarization functions (TZVPP) basis set[45] on other elements (def-TZVP (Ref. 45) on H and TZVP (Ref. 46) on I). With the use of these basis sets in the NESC/HF calculations, the EFGs of HgF, HgF_2, HgF_4, $HgCl_2$, $HgBr_2$, HgI_2, $Hg(CH_3)_2$ obtained with the use of a much larger uncontracted QZ basis set were reproduced with an average deviation of 1.7%.

The EFGs calculated at the NESC/MP2 level are in good agreement with the reference values obtained in Ref. 14 using the 4c-DC-CCSD-T method in connection with the uncontracted QZ basis set. The average deviation of the NESC/MP2 EFGs from the reference values is only 0.8%. For $Hg(CH_3)_2$ at low temperature, Arcisauskaite *et al.*[14] have reported the experimental value $\nu_Q(^{199}Hg) = 2400$ MHz. This value (no error bars were reported) is in a very good agreement with $\nu_Q(^{199}Hg) = 2414\pm43$ MHz (obtained using $eQ(^{199}Hg) = 0.675\pm0.012$ barn[14]) from the NESC/MP2 calculations. The comparison of the theoretical and experimental reference data suggests that the NESC/MP2 method in connection with the SARC and def2-TZVPP basis sets is capable of yielding accurate predictions of the EFG values for other compounds in Table IV.

As seen from Table IV, electron correlation plays an important role for the correct prediction of both EFG and contact density of the mercury atom. On average, the magnitude of V_{cc} is reduced by ~23%, which suggests that electron correlation is mandatory for an accurate description of this property.

The molecules in Table IV account for the most important oxidation states of mercury in its compounds as well as the most important structural motifs. The two parameters, $\Delta\bar{\rho}$ and V_{cc}, enable one to reliably discriminate between the different oxidation states and local chemical environments. This is illustrated in Figure 2, where the EFG values are compared with the effective contact densities. The EFG shows sufficiently high sensitivity to the local chemical environment and enables one to discriminate between compounds for which the contact density differences are nearly equal, e.g., between compounds **6** and **8**, **4** and **5**, **3** and **2**, see the upper panel of Figure 2.

For the same formal oxidation state and for the same local geometry, the V_{cc} value may vary by almost a factor of two, as seen for the compounds **2**, **4**, **5**, **6**, and **7** (formal oxidation state II, linear local geometry). There is however no simple correlation between the total charge on the mercury atom or the populations of the individual valence orbitals of

TABLE V. Results of the natural population analysis of the relaxed NESC/MP2 density matrix for mercury compounds. See header of Table IV for detail on basis sets and geometries.

Entry[a]	Molecule	Q_{Hg}[b]	n_s[c]	n_p	n_d
1	HgF	0.65	1.28	0.18	9.85
2	HgF_2	1.25	0.85	0.17	9.69
3	HgF_4	1.71	0.61	0.40	9.25
4	$HgCl_2$	0.88	0.96	0.33	9.81
5	$HgBr_2$	0.76	1.00	0.36	9.84
6	HgI_2	0.51	1.09	0.49	9.87
7	$Hg(CH_3)_2$	0.88	1.15	0.20	9.75
8	$Hg(SH)_4$	0.47	0.90	0.91	9.67
9	$Hg(SH)_4^{2-}$	0.49	0.73	0.83	9.90
10	$Hg(cys)_2$	0.69	1.12	0.33	9.83
11	$HgCl_2$-crown-S_6	0.51	0.88	0.70	9.85

[a]Number of entry in Figure 2.
[b]Total natural charge on the mercury atom.
[c]Populations of the valence orbitals of mercury.

mercury with the calculated V_{cc} values. Table V lists the results of the natural population analysis of the NESC/MP2 relaxed density matrix for the mercury compounds. Linear regression analyses of the EFG values against Q_{Hg}, n_s, n_p, or n_d do not reveal any significant correlation. It is only the combined electron population of the 6*p*-orbitals and the hole population of the 5d-orbitals of mercury that indicates moderate correlation ($r^2 = 0.4069$) with the V_{cc} values, see Figure 3. It is noteworthy that, for the same oxidation state of the mercury atom, the correlation improves noticeably. Thus, if only Hg(II) species are analyzed, Pearson's correlation coefficient r^2 increases to 0.6724. The existence of such a correlation is not at all surprising as the EFG depends on the deformation (i.e., quadrupole) density near the atomic nucleus.[48,49] Interestingly, the contact density also shows a noticeable correlation with the deformation population ($n_p^e + n_d^h$), which, most likely, occurs due to the combined effect of the depletion of the electron density from the 6*s*- and 5*d*-orbitals of mercury and of the changes of the screening due to the population of the 6*p*-orbital of mercury.

Mercury is of substantial interest for experimental investigations due to its biological activity and, in particular, its toxicity. Mercury has a high affinity to thiol ligands and to biological and organic molecules containing sulfur. Mercury in biological compounds can be analyzed using a variety of experimental techniques, in particular, the ^{199m}Hg PAC spectroscopy,[50] which measures the nuclear quadrupole interaction. We have therefore evaluated the value of the NQCC ν_Q for the $Hg(cys)_2$ complex (see Figure 1), for which ν_Q and the asymmetry parameter η are know from the experiments.[51] Using 0.675±0.012 barn for the quadrupole moment of ^{199}Hg,[14] NQCC for $Hg(cys)_2$ from NESC/MP2 is 1486±26 MHz in a reasonable agreement with the experimental value of 1410±20 MHz.[51] The asymmetry parameter $\eta = 0.033$ from the NESC/MP2 calculation is somewhat underestimated as compared to the experimental value of 0.15±0.02.[51] Most likely, this is the consequence of using the geometry of $Hg(cys)_2$ optimized in a NESC/B3LYP calculation without the inclusion of environmental effects.

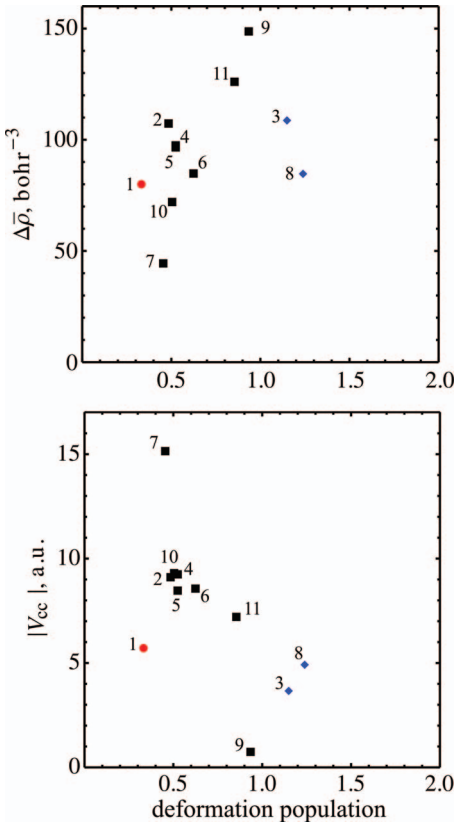

FIG. 3. Electric field gradient V_{cc} (in a.u., lower panel) and the effective contact density $\Delta\bar{\rho} = \bar{\rho}_{Hg} - \bar{\rho}_{Mol}$ (in bohr^{-3}, upper panel) vs. deformation density for mercury compounds calculated using the NESC/MP2 method. Black squares label the Hg(II) compounds, red dot the Hg(I) compound, and blue diamonds the Hg(IV) compounds.

For instance, when using the geometry optimized for this complex utilizing the NESC/B2PLYP-D method, the values $\nu_Q = 1546\pm27$ MHz and $\eta = 0.31$ were obtained. This shows a high sensitivity of the EFG tensor to the molecular geometry, which can be used for the interpretation of the experimental NQR or PAC data on biological compounds of mercury and other elements. For a more accurate comparison with experiment, corrections for the intermolecular interaction and vibrational averaging need to be taken into account. In this regard, the analytic second derivatives formalism for the NESC method[21] can be used for obtaining the derivatives of EFGs with respect to the vibrational normal modes as required for computing the vibrationally corrected NQCCs.[52]

V. CONCLUSIONS

Based on the analytic derivatives formalism for the NESC method, we have developed and presented a new computational scheme for the calculation of the electric field gradient at the atomic nuclei. The use of the NESC analytic derivatives technique provides a computationally simple and conceptually transparent algorithm that can be used for the calculation of EFGs at heavy atoms in large inorganic and bio-inorganic molecules.

The method developed has been tested in the calculation of the EFG values of a series of hydrogen halides HX

(X = F, Cl, Br, I, At) and of a series of inorganic and organometallic mercury compounds. Comparison with the available reference data, both theoretical and experimental, reveals a high accuracy of the method developed, which is capable of reproducing the reference values within a few percent. Application of the NESC/MP2 formalism to obtain the EFG values in mercury molecules reveals a high sensitivity of the calculated EFG values with regard to the electronic structure. In combination with the previously developed analytic approach for the calculation of the contact densities at the nuclei of heavy elements, the method presented is promising in connection with the theoretical interpretation and simulation of various spectra including Mössbauer spectra, NMR, NQR, and PAC spectra of compounds containing heavy elements.

[1] E. A. C. Lucken, *Nuclear Quadrupole Coupling Constants* (Academic, London, 1969).
[2] P. Gütlich, E. Bill, and A. Trautwein, *Mössbauer Spectroscopy and Transition Metal Chemistry: Fundamentals and Applications* (Springer, Heidelberg, 2011).
[3] E. A. C. Lucken *Advances in Nuclear Quadrupole Resonance*, edited by J. A. S. Smith (Wiley, New York, 1990), p. 86.
[4] R. V. Parish, *NMR, NQR, EPR, and Mössbauer Spectroscopy in Inorganic Chemistry*, Ellis Horwood Series in Inorganic Chemistry (E. Horwood, Chichester, 1990).
[5] H. Haas and D. A. Shirley, J. Chem. Phys. **58**, 3339 (1973).
[6] F. Neese, *Electron Paramagnetic Resonance*, edited by B. C. Gilbert, M. J. Davies, and D. M. Murphy (The Royal Society of Chemistry, Cambridge, 2007), Vol. 20, pp. 73–95.
[7] E. van Lenthe and E. J. Baerends, J. Chem. Phys. **112**, 8279 (2000).
[8] S. Stopkowitz and J. Gauss, J. Chem. Phys. **134**, 204106 (2011).
[9] F. Neese, A. Wolf, T. Fleig, M. Reiher, and B. A. Hess, J. Chem. Phys. **122**, 204107 (2005).
[10] R. Mastalerz, G. Barone, R. Lindh, and M. Reiher, J. Chem. Phys. **127**, 074105 (2007).
[11] M. Pernpointner and L. Visscher, J. Chem. Phys. **114**, 10389 (2001).
[12] J. N. P. van Stralen and L. Visscher, J. Chem. Phys. **117**, 3103 (2002).
[13] L. Belpassi, F. Tarantelli, A. Sgamellotti, H. M. Quiney, J. N. P. van Stralen, and L. Visscher, J. Chem. Phys. **126**, 064314 (2007).
[14] V. Arcisauskaite, S. Knecht, S. P. A. Sauer, and L. Hemmingsen, Phys. Chem. Chem. Phys. **14**, 2651 (2012).
[15] M. Pernpointner, P. Schwerdtfeger, and B. A. Hess, Int. J. Quantum Chem. **76**, 371 (2000).
[16] W. Zou, M. Filatov, and D. Cremer, J. Chem. Phys. **134**, 244117 (2011).
[17] M. Filatov, W. Zou, and D. Cremer, J. Chem. Theor. Comput. **8**, 875 (2012).
[18] M. Filatov, W. Zou, and D. Cremer, J. Phys. Chem. A **116**, 3481 (2012).
[19] K. G. Dyall, J. Chem. Phys. **106**, 9618 (1997).
[20] W. Zou, M. Filatov, and D. Cremer, Theor. Chem. Acc. **130**, 633 (2011).
[21] W. Zou, M. Filatov, and D. Cremer, "Development, Implementation, and Application of an Analytic Second Derivative Formalism for the Normalized Elimination of the Small Component Method," J. Chem. Theory Comput. (in press).
[22] E. N. Kaufmann and R. J. Vianden, Rev. Mod. Phys. **51**, 161 (1979).
[23] D. Cremer and F. Krüger, J. Phys. Chem. **96**, 3239 (1991).
[24] H. Hellmann, *Einführung in die Quantenchemie* (F. Deuticke, Leipzig, 1937), p. 285.
[25] R. P. Feynman, Phys. Rev. **56**, 340 (1939).
[26] K. G. Dyall, J. Comp. Chem. **23**, 786 (2002).
[27] P. A. M. Dirac, Proc. R. Soc. London A **117**, 610 (1928).
[28] T. D. Newton and E. P. Wigner, Rev. Mod. Phys. **21**, 400 (1949).
[29] L. L. Foldy and S. A. Wouthuysen, Phys. Rev. **78**, 29 (1950).
[30] B. Swirles, Proc. R. Soc. London A **152**, 625 (1935).
[31] P. Hafner, J. Phys. B **13**, 3297 (1980).
[32] A. C. Hennum, W. Klopper, and T. Helgaker, J. Chem. Phys. **115**, 7356 (2001).
[33] H. Taketa, S. Huzinaga, and K. O-ohata, J. Phys. Soc. Japan **21**, 2313 (1966).
[34] E. Kraka, M. Filatov, J. Gräfenstein, W. Zou, H. Joo, D. Izotov, J. Gauss, Y. He, A. Wu, V. Polo, L. Olsson, Z. Konkoli, Z. He, and D. Cremer, *COLOGNE2011* (Southern Methodist University, Dallas, TX, 2011).
[35] L. Visscher and K. G. Dyall, At. Data Nucl. Data Tables **67**, 207 (1997).
[36] G. Gabrielse, D. Hanneke, T. Kinoshita, M. Nio, and B. Odom, Phys. Rev. Lett. **97**, 030802 (2006).
[37] L. Cheng and J. Gauss, J. Chem. Phys. **135**, 084114 (2011).
[38] C. van Wüllen, J. Chem. Phys. **120**, 7307 (2004).
[39] M. Filatov and D. Cremer, J. Chem. Phys. **123**, 124101 (2005).
[40] N. J. Taylor and A. J. Carty, J. Am. Chem. Soc. **99**, 6143 (1977).
[41] T. Tsuchiya, T. Shimizu, K. Hirabayashi, and N. Kamaigata, J. Org. Chem. **68**, 3480 (2003).
[42] G. J. Grant, Struct. Bonding (Berlin) **120**, 107 (2006).
[43] D. A. Pantazis, X.-Y. Chen, C. R. Landis, and F. Neese, J. Chem. Theory Comput. **4**, 908 (2008).
[44] R. Krishnan, J. S. Binkley, and J. A. Seeger, and R. Pople, J. Chem. Phys. **72**, 650 (1980).
[45] F. Weigend and R. Ahlrichs, Phys. Chem. Chem. Phys **7**, 3297 (2005).
[46] R. Ahlrichs and K. May, Phys. Chem. Chem. Phys. **2**, 943 (2000).
[47] S. Knecht, S. Fux, R. Van Meer, L. Visscher, M. Reiher, and T. Saue, Theor. Chem. Acc. **129**, 631 (2011).
[48] F. L. Hirshfeld, Acta Cryst. **B27**, 769 (1971).
[49] D. Schwarzenbach and N. Thong, Acta Cryst. A **35**, 652 (1979).
[50] L. Hemmingsen, K. N. Sas, and E. Danielsen, Chem. Rev. **104**, 4027 (2004).
[51] O. Iranzo, P. W. Thulstrup, S.-b. Ryu, L. Hemmingsen, and V. L. Pecoraro, Chem.-Eur. J. **13**, 9178 (2007).
[52] A. D. Buckingham, J. Chem. Phys. **36**, 3096 (1962).